Cell Tissue Res (1985) 240:159–168

Cell and Tissue Research

Morphometric analysis of the isolated calcium-tolerant cardiac myocyte

Organelle volumes, sarcomere length, plasma membrane surface folds, and intramembrane particle density and distribution

N.J. Severs, A.M. Slade, T. Powell[1], V.W. Twist[1], and G.E. Jones[2]

Department of Cardiac Medicine, Cardiothoracic Institute, London;
[1] Department of Physics as Applied to Medicine, Middlesex Hospital Medical School, London;
[2] Department of Biology, Queen Elizabeth College, London, Great Britain

Summary. Using morphometric analysis of thin sections and freeze-fracture replicas, the ultrastructure of isolated rat myocytes prepared by collagenase digestion (Powell et al. 1980) was compared with that of myocytes fixed by perfusion of intact myocardium. The volumes of myofibrils, mitochondria, nuclei, sarcoplasmic reticulum and lipid droplets in the isolated myocytes did not differ from those of their counterparts in the intact heart, but the volume occupied by transverse tubules was apparently reduced. The isolated cells had significantly shorter sarcomeres than did cells in the intact tissue, and this was associated with an altered topography of plasma membrane surface folds at the level of the Z-lines. Plasma membrane intramembrane particles were randomly distributed and showed the same numerical density on the E-faces of both isolated and intact-heart myocytes. However, P-face particle density was slightly reduced in the isolated cells. It is concluded that the few differences detected in the isolated cells do not reflect any fundamental derangement of their properties.

Key words: Myocardium – Isolated myocyte – Plasma membrane – Intramembrane particle analysis – Freeze-fracture – Morphometry – Rat

Isolated cardiac myocytes provide a useful model system for the investigation of myocardial function at the cellular level (Dow et al. 1981a, b). Using thin section and freeze-fracture electron microscopy, we have previously investigated the ultrastructural features of calcium-tolerant myocytes isolated from the adult rat heart, and discussed our findings in relation to the functional properties shown by these cells (Severs et al. 1982). After isolation of myocytes by the method of Powell et al. (1980), all the normal features of cellular structure appear well preserved and no irreversible damage appears to be sustained as a result of separation of the intercalated discs. However, although the ultrastructure of these cells appears qualitatively similar to that of myocytes in the intact heart, the possibility that the isolation process leads to quantitative changes in the cell's ultrastructural components has not previously been investigated. The purpose of the present study was to examine this possibility in detail by applying morphometric techniques to analyse (i) subcellular component and organelle volumes by thin-section electron microscopy, and (ii) plasma membrane topography and macromolecular structure from freeze-fracture replicas. Particular emphasis is given to new information on sarcomere length, plasma membrane surface folds and intramembrane particle density and distribution.

Send offprint requests to: Dr. N.J. Severs, Department of Cardiac Medicine, Cardiothoracic Institute, 2, Beaumont Street, London, W1N 2DX, Great Britain.

Materials and methods

A. Preparation of isolated myocytes and intact myocardial tissue

Hearts were obtained from adult female Sprague-Dawley rats weighing 250–300 g. The animals were maintained on a standard chow diet with tap water available ad libitum. Four hearts were used for the preparation of isolated myocytes, and a further four for the examination of myocytes in intact tissue.

Suspensions of purified cardiac myocytes were obtained by retrograde perfusion of the hearts through the aorta (Langendorff 1895) with crude collagenase in low-calcium Krebs-Ringer bicarbonate buffer as described in detail previously (Powell et al. 1980). The isolated cells were fixed by adding 1 volume of the myocyte suspension to 4 volumes of 2% glutaraldehyde in either 1/3 strength Krebs buffer or 0.1 M sodium cacodylate buffer (pH 7.3) at 37° C.

Whole hearts were perfusion-fixed by the Langendorff technique with cacodylate-buffered 2% glutaraldehyde at a continuously monitored mean pressure of 8KPa (60 mm Hg) at 37° C as described by Nayler et al. (1978).

After initial fixation, both the isolated myocyte preparations and multiple small samples of left ventricular tissue cut from the perfusion-fixed hearts were transferred to fresh glutaraldehyde fixative at room temperature for 2 h. At the end of this period, the samples from each of the four isolated myocyte preparations and those from each of the four hearts were split into two batches, one for thin section electron microscopy and one for freeze-fracture.

B. Electron microscopy

All samples for thin sectioning were rinsed in 0.1 M sodium cacodylate buffer, post-fixed in cacodylate-buffered 1% OsO_4 at 4° C for 2 h, en-bloc stained with saturated aque-

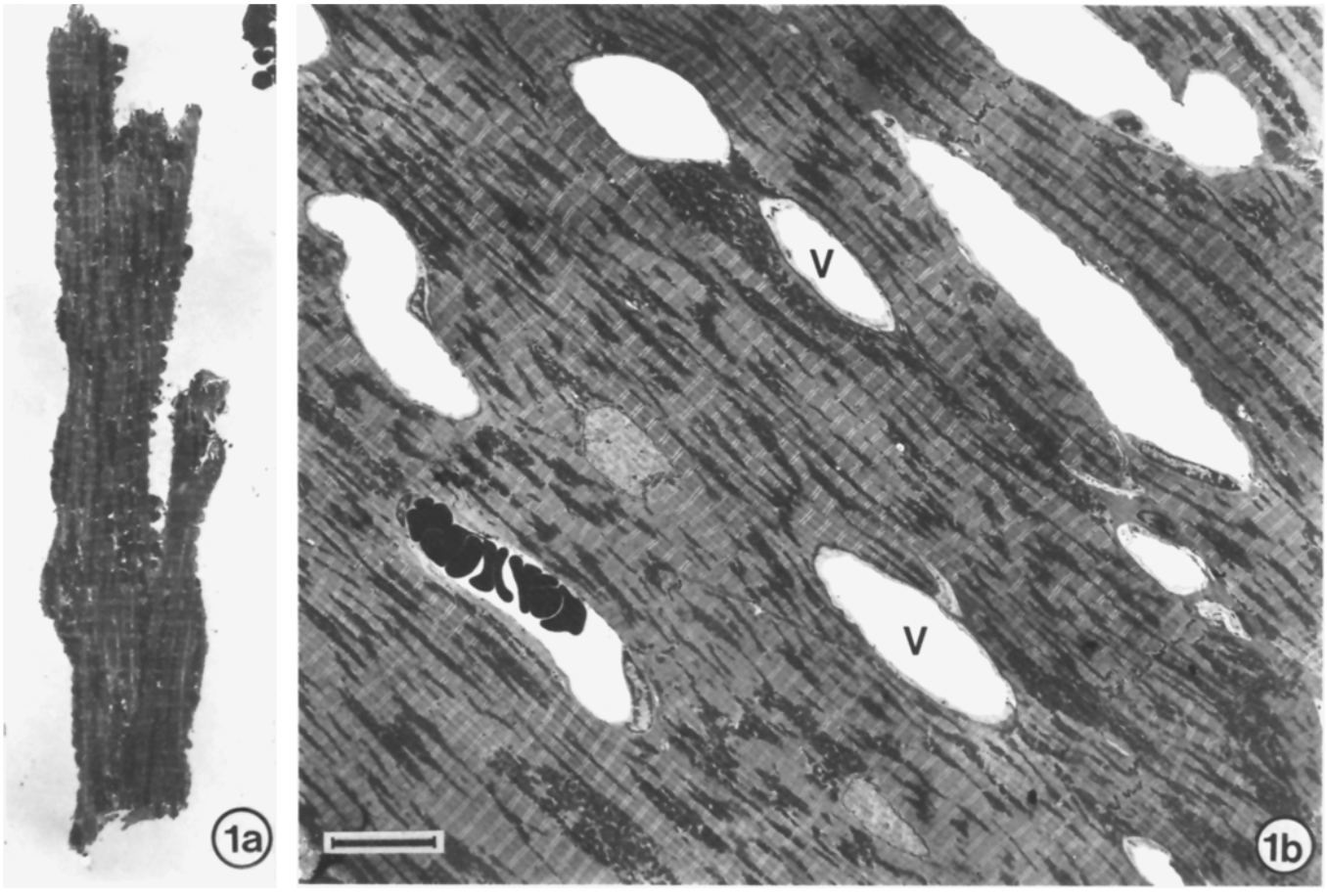

Fig. 1 a, b. Survey thin section views of an isolated 'rod-shaped' myocyte (**a**) and intact myocardial tissue (**b**) from rat heart. *V* capillaries and small blood vessels. × 1350. Bar = 10 μm

ous uranyl acetate for 1 h at room temperature, dehydrated in ethanol and embedded in Araldite via propylene oxide. Sections were prepared using an LKB III ultramicrotome, and some were further stained with uranyl acetate and lead citrate.

For freeze-fracture, samples were gradually infiltrated with glycerol in cacodylate buffer to a final glycerol concentration of 25% over a period of 70–80 min. They were then mounted and frozen by immersion into liquid nitrogen-cooled Freon 12 or propane. Freeze-fracturing was carried out either by microtome or by using a double replica device in a Balzers BAF 400T unit at a temperature of between −110 and −115° C and at a vacuum of 5×10^{-7} mbar or better. Replicas were routinely made immediately after fracturing, though in some runs (not used for intramembrane particle analysis) the specimens were briefly etched first. The replicas were cleaned in 40% chromic acid and rinsed in distilled water. A minimum of six replicas (i.e., six specimens) were prepared from each heart and from each isolated myocyte preparation.

Thin sections and freeze-fracture replicas were examined and images recorded using a Philips EM 301 electron microscope.

C. Morphometric analysis

i) Myocyte organelle and subcellular component volumes. Ribbons of longitudinally-sectioned cells were prepared from three blocks from each isolated myocyte preparation and from three blocks from each heart. One section only per ribbon was selected for image recording, and the grid bars were used as a reference system to avoid operator bias (Weibel 1969). Ten exposures were taken from each section at the upper left-hand corners of the fields framed by the grid bars. The negatives were printed at a final magnification of × 30000 with a superimposed lattice grid of 16 mm 'd' spacing. The volumes of subcellular components were determined by point-counting according to Weibel (1969) using a total of 120 micrographs from the isolated myocyte preparations and a further 120 micrographs from intact tissue. The following components were measured: myofibrils, mitochondria, nuclei, transverse tubules, sarcoplasmic reticulum and lipid droplets. Points occurring over cytoplasmic space and structures which could not be identified were placed in the category 'other'.

ii) Sarcomere lengths. Survey micrographs from each sample were printed to a final magnification of × 30000. On thin section micrographs of cells cut in precise longitudinal section, measurements were made of the distance between Z-lines at the beginning and end of a series of sarcomeres, and the average sarcomere length of each cell determined. Sixteen cells from intact tissue, and a further sixteen from isolated myocyte preparations, were measured in this way. Similar measurements were made on freeze-fracture views of the plasma membrane, using the periodic distribution of surface folds and/or transverse tubules as markers of the Z-band positions. Only the more clearly defined series

Table 1. Comparison of percentage volumes[a] (± SEM, $n=4$) of organelles and subcellular components in isolated myocytes and myocytes of intact tissue

Myocyte component	Isolated myocytes	Myocytes of intact tissue
Myofibrils	53.3±1.4	54.8±0.5
Mitochondria	34.0±1.2	37.5±1.0
Nucleus	4.2±0.6	2.5±0.5
Transverse tubules	1.7±0.2*	3.2±0.3*
Sarcoplasmic reticulum	1.0±0.3	0.6±0.2
Lipid droplets	0.3±0.05	0.2±0.04
'Other'	5.5±0.9*	1.2±0.4*

* Indicates significantly different at $P<0.05$. (The significant difference recorded in the category 'Other' reflects the presence of more imperfections concealing recognisable structure in the isolated myocyte sections than in the intact-heart sections analysed)

[a] Group means were compared using Students *t*-test

of surface folds were selected (e.g., similar to those shown in Fig. 3), and the measurements made to the mid-line bisecting the fold. In intact myocardium, this mid-line corresponds to the central ridge of the fold (see Results).

iii) Numerical density and distribution of intramembrane particles. En-face views of the freeze-fractured myocyte plasmamembrane were recorded at a magnification of ×28000. From a pool of these images, six P-face views and six E-face views (each representing a different cell) were selected from each of the four isolated myocyte preparations and from each of the four hearts providing intact tissue samples. The criteria for selection were minimal curvature of the membrane and optimal replica quality and shadow density. The micrographs were printed at a final magnification of ×200000 and a 10×10 cm test grid (sub-divided into 100×1 cm^2 squares) superimposed over each print. The number of particles visible in each of the squares was recorded using a Kontron digitizer tablet and a MOP I microprocessor interfaced with a Commodore PET 3032 equipped with a ROM designed for this combination of instruments (Jones et al. 1983). The analysis was performed 'blind' to exclude the possibility of operator bias. Intramembrane particles of less than 5 nm diameter were excluded. Intramembrane particle density (i.e., number of particles μm^{-2}) and the coefficient of dispersion were determined for each set of six prints. The coefficient of dispersion gives a measure of particle distribution in relation to the Poisson (random) hypothesis (Pauli et al. 1978). In a random distribution, the variance and mean are equal; the ratio of variance to mean, or coefficient of dispersion, is thus 1.0. As detailed by Pauli et al. (1978), values for the coefficient of dispersion below 0.67 indicate statistically significant ordering of particles, those above 1.4 indicate statistically significant aggregation, and those falling between 0.67 and 1.4 indicated statistically significant randomness at $P<0.01$.

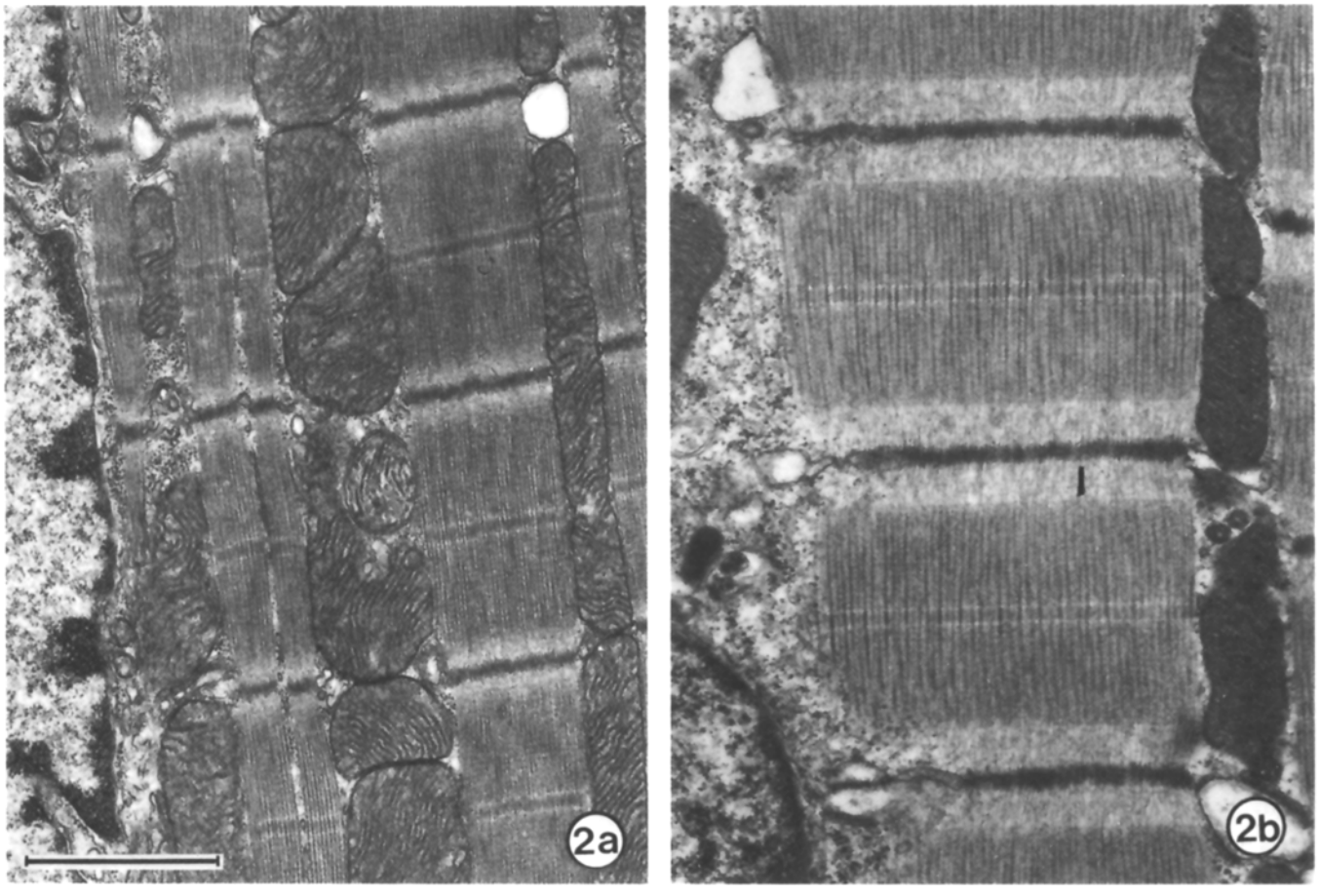

Fig. 2a, b. Thin section comparison of the contractile apparatus in an isolated myocyte (**a**) and a myocyte from intact tissue (**b**). Note wider I-bands (*I*) in the latter. ×25700. Bar = 1 μm

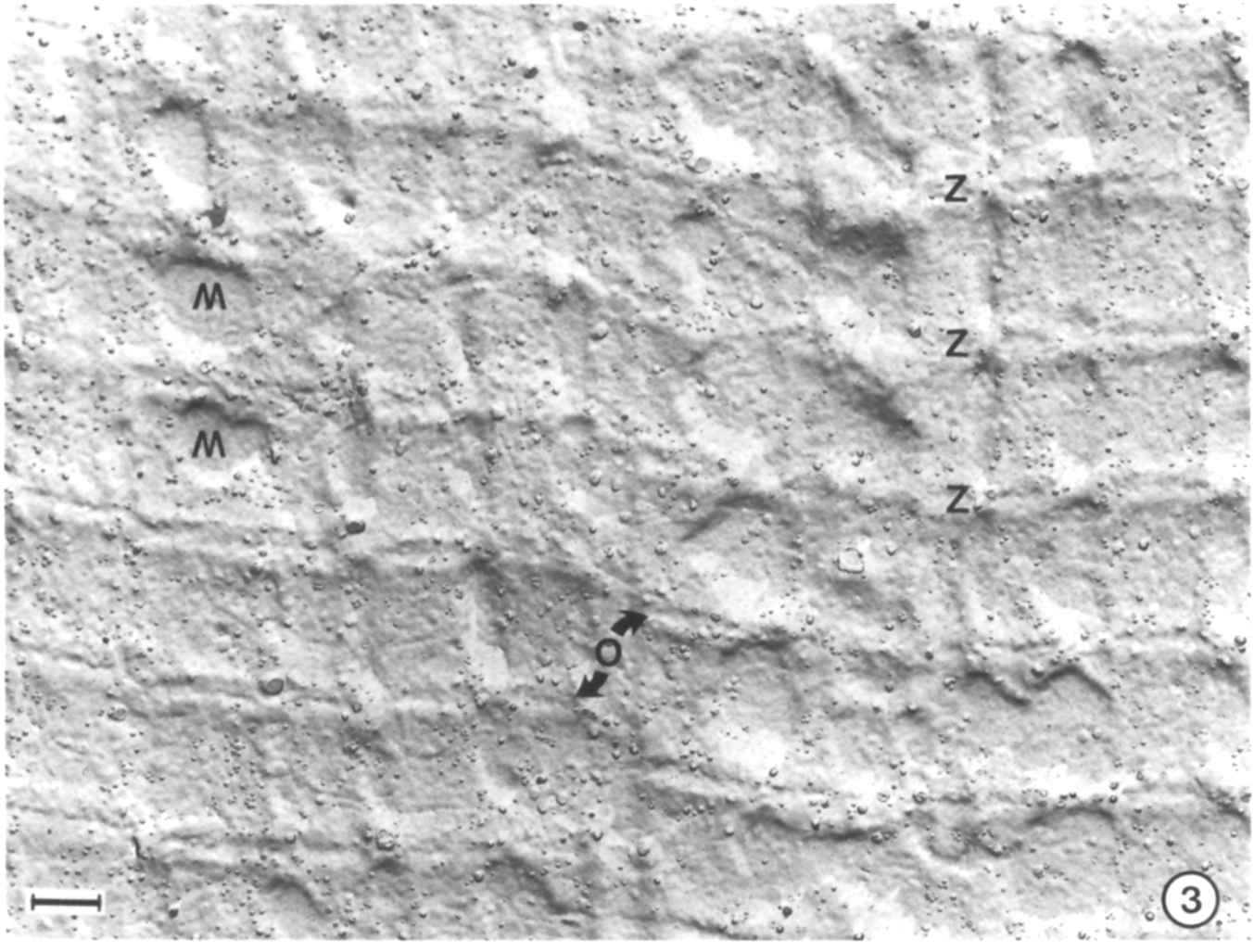

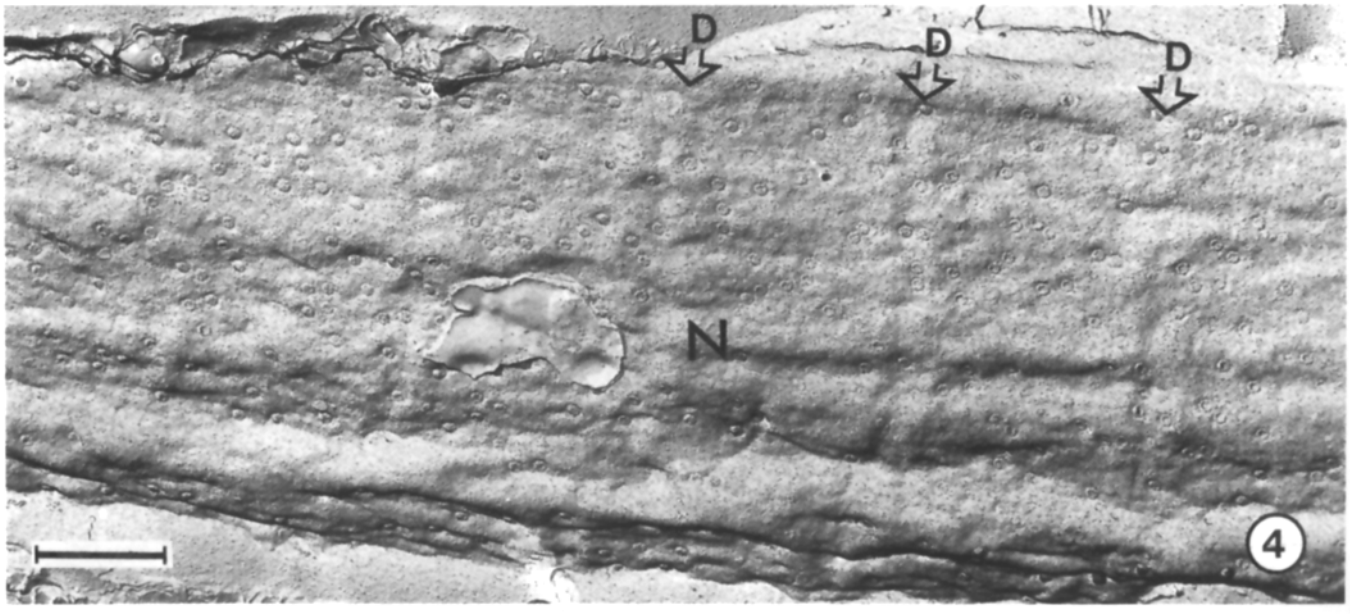

Fig. 3. Freeze-fractured plasma membrane (E-face view) of a myocyte from intact tissue. Note doublet appearance of Z-folds (*Z*). *O* offset Z-folds; *M* imprints of mitochondria. ×10300. Bar = 1 μm

Fig. 4. Freeze-fractured nuclear membrane (*N*) from an intact-tissue myocyte. Periodic deformations (*D*) circumscribe the nucleus at the level of the Z-bands. ×16700. Bar = 1 μm

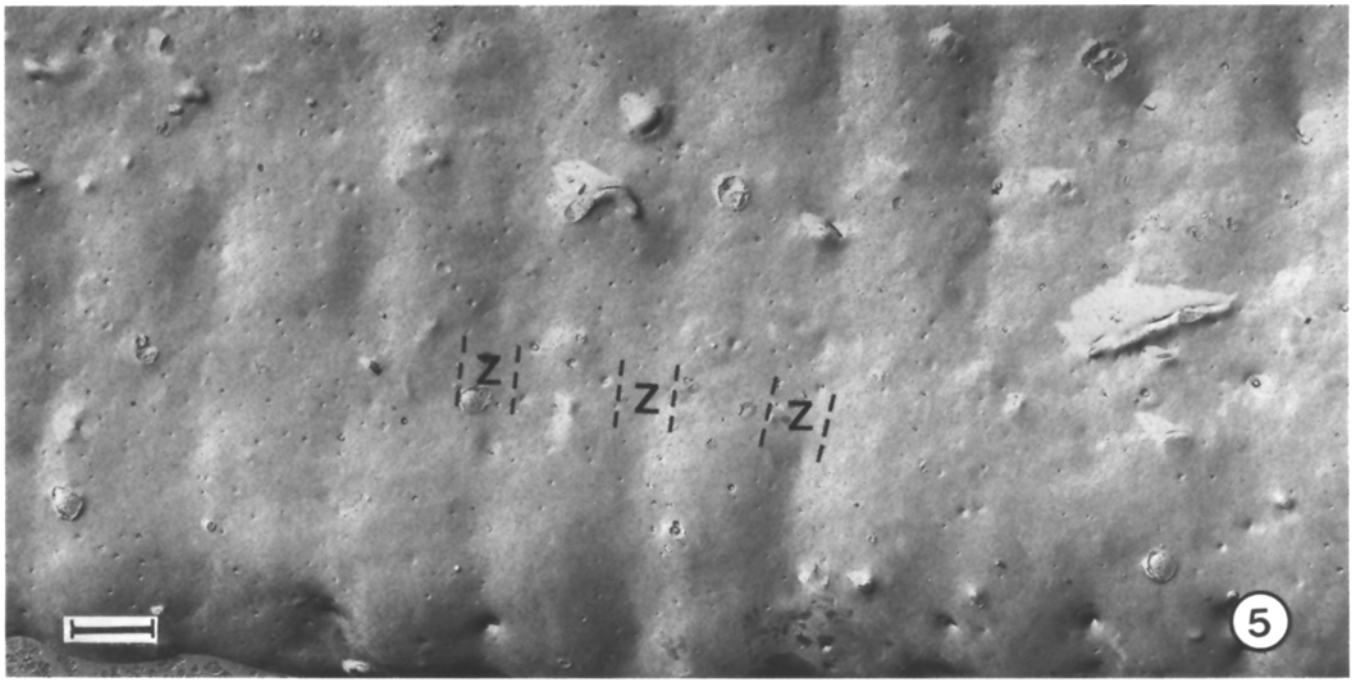

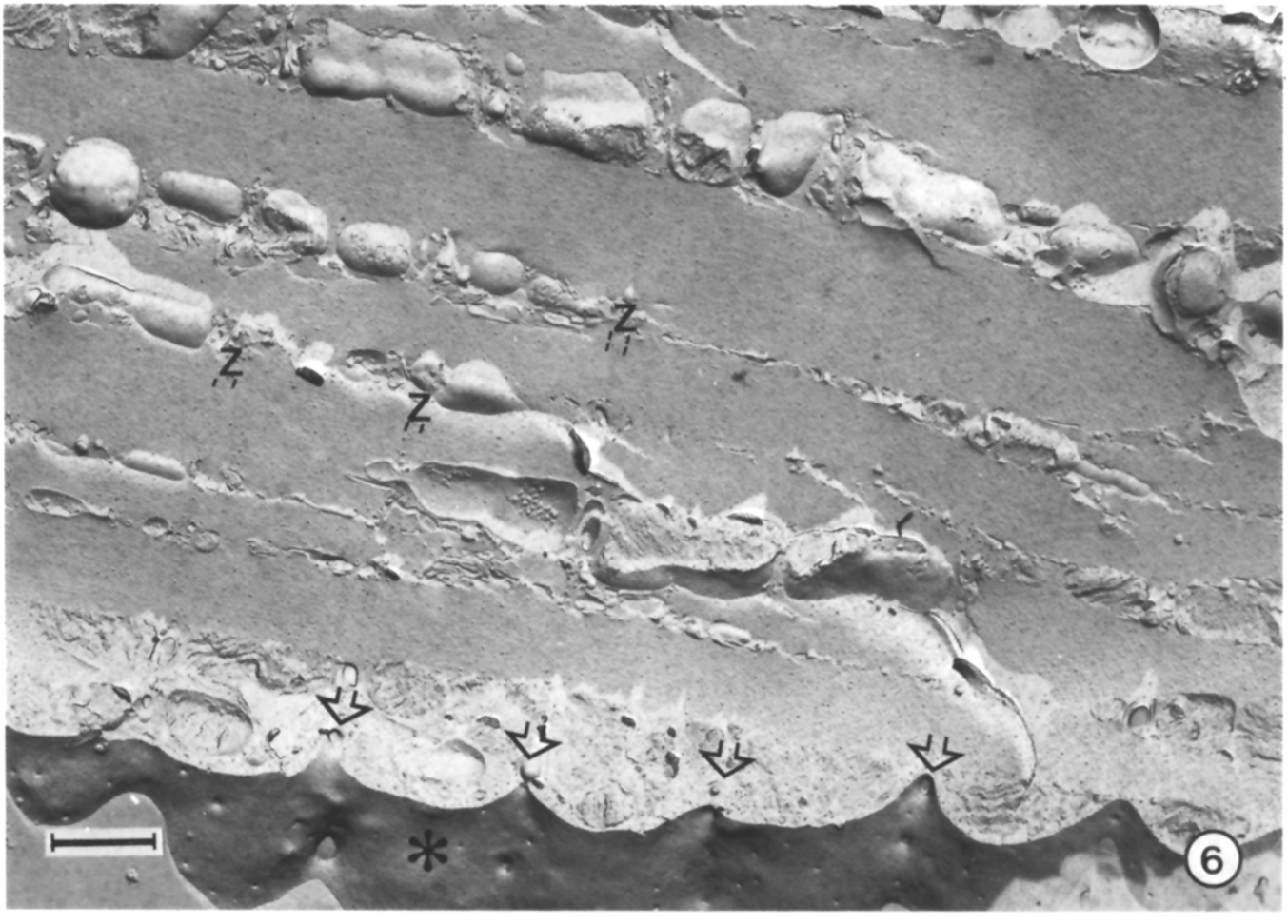

Fig. 5. Freeze-fractured plasma membrane (P-face view) from an isolated myocyte. In contrast to Fig. 3, each Z-fold (*Z*) appears as a single broad depression. ×10300. Bar = 1 μm

Fig. 6. Freeze-fractured isolated myocyte showing a cross-fracture view of the cell interior together with a small portion of the plasma membrane (*) in planar (P-face) view. Z-lines (*Z*) are clearly aligned with the indentations of Z-folds (*arrowheads*). ×14000. Bar = 1 μm

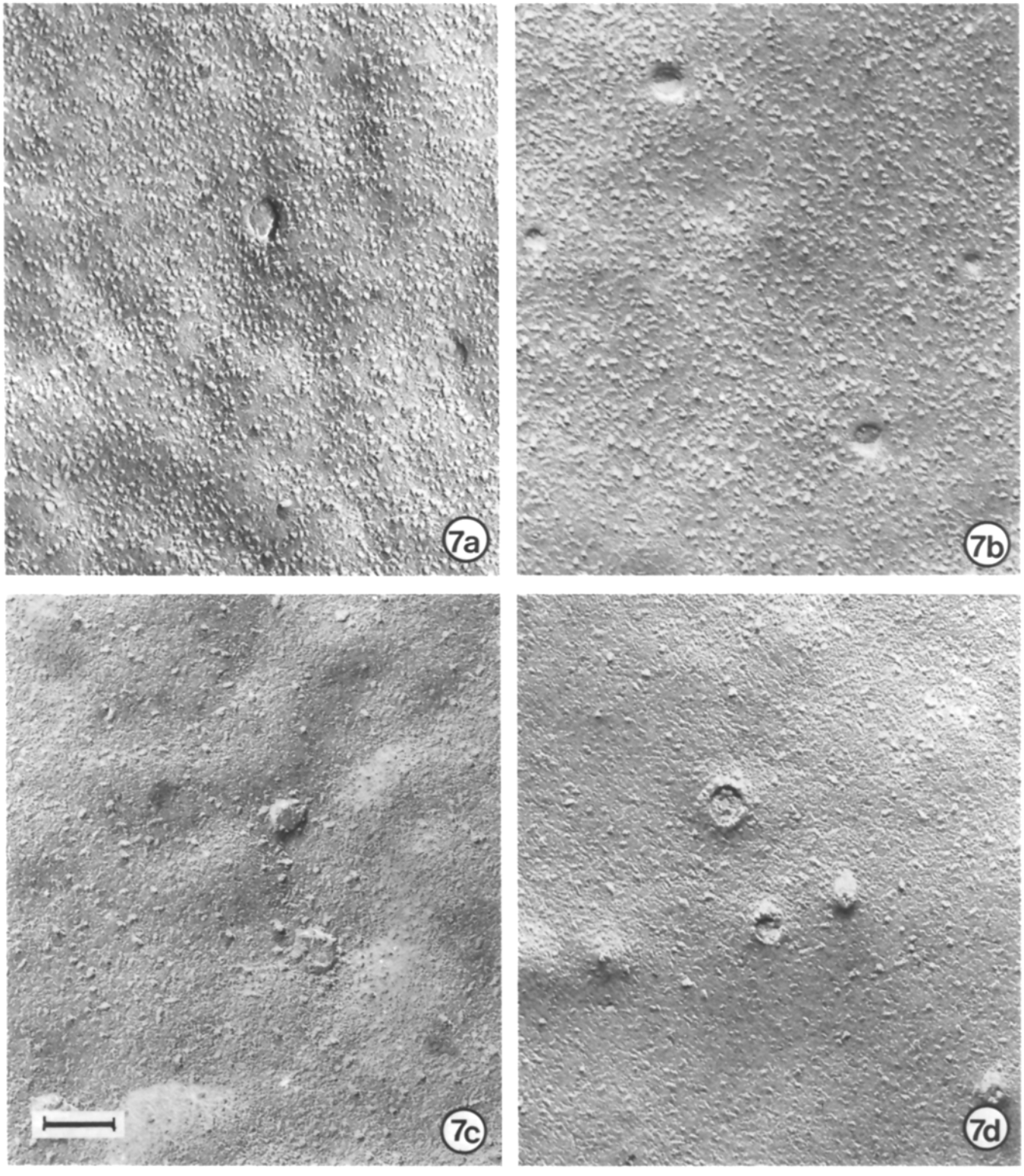

Fig. 7. Examples of freeze-fractured myocyte plasma membranes giving typical views of intramembrane particle density and distribution (**a**) P-face, intact-tissue myocyte; (**b**) P-face, isolated myocyte; (**c**) E-face, intact-tissue myocyte; (**d**) E-face, isolated myocyte. ×120400. Bar = 100 nm

Results

Fig. 1a illustrates the typical thin-section appearance of an individual 'rod-shaped' myocyte after isolation by the method of Powell et al. (1980). For comparison, a survey view of intact myocardium is shown in Fig. 1b. Inspection of these micrographs confirms that the ultrastructural features of the isolated myocytes used in the present study closely resemble those of their counterparts in intact tissue, as previously reported in similar preparations (Severs et al. 1982). Comparison of the volumes of the principal organelles and components of the cells (Table 1) demonstrates

that this qualitative similarity extends to the quantitative level. Statistical analysis of these data showed that, with the possible exception of transverse tubules, the organelle volumes of isolated myocytes do not differ significantly from those of myocytes in intact tissue.

Thin-section micrographs of the myofibrils reveal that the contractile apparatus of isolated myocytes is not in a fully extended condition (Fig. 2). In these cells, the I-bands are less wide and distinct, and the sarcomeres are shorter in length than those of intact myocardium fixed in a relaxed state by Langendorff perfusion. This difference is reflected in the surface topography of the plasma membrane when viewed en face by freeze-fracture (Figs. 3, 5). Relaxed rat myocytes in intact tissue (Fig. 3) characteristically display periodic folds (Z-folds overlying the Z-band positions, similar to those previously described in the rabbit myocardium (Levin and Page 1980). Individual Z-folds are typically, though not invariably, comprised of two parallel valleys separated by a central ridge (seen in reverse relief in the E-face view in Fig. 3). Vertical rows of folds delineate the longitudinal boundaries of individual myofibrils which are for the most part arranged in register side-by-side. Sometimes, however, neighbouring groups of these imprints appear offset from one another, reflecting a misalignment in the underlying myofibrils. Imprints of mitochondria pressed against the plasma membrane are also sometimes visible between consecutive Z-folds. Where these result in substantial deformation of the plasma membrane, caveolae are reduced in density compared with the surrounding membrane areas. It is interesting to note that periodic folds or deformations corresponding to the Z-band positions, are also discernible in the membranes of some nuclei (Fig. 4).

The Z-folds in the plasma membranes of isolated myocytes differ from those in the intact tissue examined, typically appearing as single broad shallow depressions without a dividing ridge (Fig. 5). In both cases, however, the Z-folds are often perforated by transverse tubule openings. In unusually favourable fractures in which the Z-band is directly visualized as a narrow cross-fractured band of concentrated particles (representing plastically-deformed products of the Z-band material) and expanses of the plasma membrane are visible alongside (Fig. 6), the precision with which the surface folds mark the Z-band positions is evident. Measurements between the surface folds or transverse tubule openings in the standard planar freeze-fracture views (in which Z-bands are not directly seen) thus provide a reliable indication of sarcomere length. Comparison of the sarcomere lengths (Table 2) reveals higher values in freeze-fracture preparations than in thin sections. Both techniques reveal a significantly shorter sarcomere length in isolated myocytes than in intact myocardium.

Inspection of the plasma membrane in high-magnification freeze-fracture view reveals no obvious difference in intramembrane particle density and distribution between isolated and intact-tissue myocytes (Fig. 7). However, quantitative analysis (Table 3) showed a slight but significant ($P=0.004$) reduction in the density of P-face particles in the isolated myocytes, though E-face particle density remained unchanged. As in most other membrane types, the density of particles on the P-faces was significantly higher ($P<0.001$) than that of the E-faces. The coefficients of dispersion in all samples but one fell between 0.82 and 1.21 indicating statistically random particle distributions (at $P<0.01$). The exception was a set of P-faces from intact tissue

Table 2. Comparative measurements of sarcomere length ($\mu m \pm$ SEM, $n=16$) in isolated myocytes and intact myocardium

Method	Isolated myocytes	Intact myocardium
Thin section	1.65 ± 0.04	1.86 ± 0.03
Freeze-fracture	1.77 ± 0.03	2.12 ± 0.03

Two-way analysis of variance showed that sarcomere lengths were significantly shorter ($P<0.05$) in isolated myocytes compared with intact myocardium, and in thin section compared with freeze-fracture for intact myocardium. In the case of isolated myocytes, the thin section and freeze-fracture values were not significantly different at the 5% level ($0.1>P>0.05$)

Table 3. Numerical density and distribution of intramembrane particles (IMP) on the plasma membranes of rat cardiac muscle cells. IMP density is given as the number of IMP per μm^2; *CD* coefficient of dispersion ($n=6$)

Sample no.	P-face	E-face
	IMP density (CD)	IMP density (CD)
Isolated myocyte preparations		
1	2461 (0.87)	1122 (1.07)
2	2429 (0.92)	1241 (0.82)
3	2453 (0.87)	1236 (1.10)
4	2541 (0.90)	1185 (1.21)
Mean $\pm$ SEM	2464 ± 18	1196 ± 28
Intact myocardium		
1	2800 (0.63)*	1177 (1.13)
2	2600 (0.82)	1219 (1.18)
3	2796 (0.86)	1211 (1.03)
4	2603 (0.90)	1154 (1.0)
Mean $\pm$ SEM	2712 ± 50	1190 ± 15

The *CD* values all indicate statistically significant randomness of *IMP* at $P<0.01$ except that marked *, which shows statistically significant ordering

(asterisk, Table 3), which with a value of 0.63 fell just within the limit of statistically significant ordering rather than randomness. This has no special biological significance; it merely indicates that the particles had a tendency to be more spread out than would be expected with a mathematically random distribution. From the point of view of membrane pathology, it is coefficients of dispersion in excess of 1.4 that are of importance, as particle aggregation is considered to be a marker of membrane damage (see Discussion).

Discussion

The quantitative ultrastructural results presented here confirm and extend our earlier descriptive ultrastructural observations on the isolated rat myocyte (Severs et al. 1982). The data for percentage volumes of myofibrils and mitochondria (Table 1) are similar to those reported in numerous other morphometric studies on intact rat myocardium (e.g., Reith and Fuchs 1973; Datta and Silver 1975; Hatt et al. 1978; David et al. 1979; McCallister et al. 1979), though for the other organelles we measured, fewer published data are available for comparison. The sarcoplasmic reticulum values, while showing no difference between isolated and intact-heart myocytes, are lower than those given

by Page and McCallister (1973) which were, furthermore, considered minimal estimates because of the difficulty in identifying this component in tangential section. Transverse tubule volume appeared to be significantly lower in our isolated myocytes than in myocytes of intact tissue, and in view of differences in contractile state (see below), this could be attributed to compression of the tubules. However, since our transverse tubule value for isolated myocytes is similar to that previously reported for intact rat tissue (Page and McCallister 1973; Stewart and Page 1978; McCallister et al. 1979), this possibility will require further investigation.

Our data on sarcomere lengths show that (i) myocytes processed for thin sectioning have shorter sarcomere lengths than those examined by freeze-fracture, (ii) this difference is more marked in intact tissue than isolated myocytes, and (iii) isolated myocytes consistently have shorter sarcomere lengths than the myocytes of intact tissue.

The sarcomere length determined in freeze-fractured isolated myocytes in the present study is similar to that measured directly in our isolated cells (1.82 ± 0.06 μm, Nash et al. 1979) and in corresponding preparations of other laboratories (Wittenberg and Robinson 1981; Robinson et al. 1981; Roos et al. 1982; see, however, Gerdes et al. 1982). The freeze-fracture data therefore appear to reflect the true values more accurately than do the thin section data, though the possibility of some shrinkage during pretreatment for freeze-fracture cannot be excluded. The problem of volume changes during processing of isolated myocytes and myocardial tissue for thin sectioning has previously been studied in detail by Gerdes et al. (1982). Although these authors detected significant alterations (notably after OsO_4 and after uranyl acetate treatment), the final dimensions of embedded isolated cells did not differ from those of unfixed cells. In contrast to the isolated cells, however, whole tissue shrank markedly (14% in length) following exposure to propylene oxide.

In seeking an explanation for the reduced sarcomere lengths found in isolated myocytes compared with intact myocardium, account must be taken of the different physical factors prevailing at the time of fixation. Indeed, comparison of sarcomere lengths in whole tissue and isolated cells is only possible if precise definitions are given to terms which, until now, have been used for multi-cellular preparations only. Thus, both the Langendorff-perfused heart and the isolated cell may be either 'at rest', 'relaxed' or 'contracting', but the mechanical loads imposed are markedly different for the two preparations. The generally accepted value of about 2.2 μm for sarcomere length at normal ventricular end-diastolic volume (Page 1974) is determined by the weight of blood in the heart, its compliance and its inotropic state. At this point in the cardiac cycle, the ventricular fibres are developing sufficient "steady-state" tension to provide the initial conditions, or pre-load, prior to systole. In the case of the isolated myocyte in suspension, the tension generated is zero, and the sarcomere length will be determined by the balance of passive and active forces present in the unloaded cell. Sarcomere lengths in isolated cells should therefore be compared only with those of whole heart in which the 'resting' tension is zero, and this length in rat papillary muscle is reported to be about 1.9 μm (Jewell 1977).

The doublet appearance of the plasma membrane folds observed in relaxed myocytes from intact rat heart (Fig. 5) is similar to that illustrated by Levin and Page (1980) in rabbit myocytes passively extended to sarcomere lengths of 2.34–2.44 μm. Why such plasma membrane folds exist in relaxed and extended cells has not hitherto been satisfactorily explained, but recent studies on the localization of the putative cytoskeleton-membrane attachment protein, vinculin (Pardo et al. 1983a, b), offer some interesting new insights into this problem. Using immunofluorescence techniques, Pardo et al. (1983a, b) have demonstrated, that in both skeletal and cardiac muscle, dense transverse patches of vinculin (termed 'costameres') are closely associated with the plasma membrane at the level of the Z-lines. In skeletal muscle, longitudinal bands of vinculin interlink the rib-like costameres, and each costamere can be resolved as a doublet flanking the Z-line (i.e., overlying the I-bands; Pardo et al. 1983a). The specific distribution of the costameres, together with the currently accepted role of vinculin as a mediator of cytoskeleton attachment to membranes (Geiger et al. 1980, 1981), has led to the proposal that vinculin physically anchors the Z-discs to the cell surface, thereby mechanically integrating the contractile machinery and the plasma membrane (Pardo et al. 1983a, b).

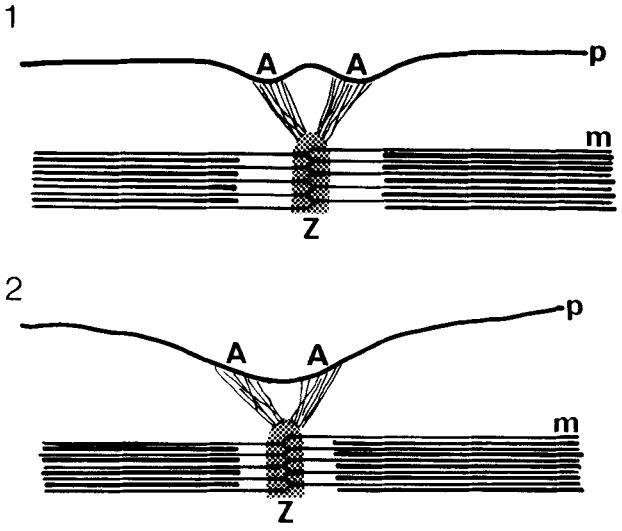

Fig. 8. Diagrams illustrating possible relationship between morphology of plasma membrane Z-folds and anchorage sites (*A*) for vinculin and other membrane-attachment proteins in (*1*) a myocyte from perfusion-fixed heart and (*2*) an isolated myocyte. These diagrams correspond respectively to the en-face freeze-fracture views in Figs. 3 and 5. *Z* Z-band; *m* myofibril; *p* plasma membrane

That costameres and surface fold doublets are intimately related is evident from their correspondence in location, periodicity and distribution. This correspondence extends to the presence of longitudinal elements, and staggered patterns of transverse elements where the underlying myofibrils are misaligned. We therefore interpret the twin depressions of the surface folds as the anchorage sites of vinculin and believe that they are generated by the tension of these proteins pulling on the membrane as depicted in Fig. 8. The replacement of the doublet of depressions by a single broad depression at shorter sarcomere lengths, as observed in isolated myocytes, could then be explained by alterations in the forces acting on the attachment sites which arise as the cell contracts.

The intramembrane particle densities recorded on the plasma membrane fracture faces of myocytes in intact rat

myocardium (Table 3) exceed those reported in earlier studies of the myocardia of a variety of mammalian species (Rayns et al. 1968; Fry et al. 1979; Gros et al. 1980; Frank et al. 1980, 1982), including the rat (Bullock et al. 1981) in which similar standard counting methods were used. However, in a recent systematic investigation using stereo-imaging (Kordylewski et al. 1983), the P-face values obtained were at least two-fold those of the earlier studies. Apart from this difference, attributable to the detection by stereo-viewing of otherwise inconspicuous particulate detail, a notable feature of all the data is the lack of agreement between the results reported from different laboratories. The principal sources of this variation are probably (i) differences in the technical procedures used for freeze-fracture (e.g., fixation method, adequacy of protection from condensation contamination, replica quality etc), and (ii) differences in the criteria adopted as to precisely which structures are classified as intramembrane particles. As discussed by Shotton (1982) and Kordylewski et al. (1983), close inspection of good quality micrographs reveals a rich variety in size, shape, height and prominence of particulate-like detail; hence even assuming the feasibility of ensuring standardised optimal procedures in all laboratories, uniformity in the final data of different research groups might still prove difficult to achieve.

Although direct comparisons of the absolute intramembrane particle values reported from different research groups would seem to be of dubious significance, the overall patterns of experimentally-induced change do nevertheless appear to be reproducible. A decrease in the numerical density and/or aggregation of intramembrane particles is widely believed to characterise early functional damage to the cardiac muscle cell plasma membrane, and such alterations have been reported in response to myocardial ischaemia and reperfusion (Ashraf and Halverson 1977), anoxia and reoxygenation (Frank et al. 1980), and calcium depletion and repletion (Ashraf 1979; Fry et al. 1979; Frank et al. 1982; see, however, Bullock et al. 1981). Since the procedure for isolating myocytes involves their exposure to calcium-deficient solutions, the isolated cells might be expected to show similar alterations in plasma membrane structure to those of calcium-depleted cells in intact tissue. Using a preparation of rabbit myocytes dissociated by perfusion with solutions containing EGTA and hyaluronidase, Fry et al. (1979) found that this did indeed appear to be the case. Their cells, which were not calcium-tolerant, revealed a marked reduction in an aggregation of P-face particles. Our calcium-tolerant cells, by contrast, showed only a slight reduction in P-face particles, no alteration in the number of E-face particles, and no evidence of particle aggregation even after analysis by sensitive statistical tests.

Acknowledgements. This work was supported by British Heart Foundation grants to N.J. Severs and T. Powell.

References

Ashraf M (1979) Correlated studies in sarcolemmal ultrastructure, permeability, and loss of intracellular enzymes in the isolated heart perfused with calcium-free medium. Am J Pathol 97:411–432

Ashraf M, Halverson C (1977) Structural changes in freeze-fractured sarcolemma of the ischemic myocardium. Am J Pathol 88:583–594

Bullock GR, Kemmenoe B, Baker JE, Hearse DJ (1981) Hypothermia and the calcium paradox: a model for microcomputer analysis of freeze-fractured cardiac membranes. J Mol Cell Cardiol 13 (suppl 1):12 (abstract)

Datta BN, Silver MD (1975) Cardiomegaly in chronic anemia in rats. An experimental study including ultrastructural, histometric and stereologic observations. Lab Invest 32:503–514

David M, Meyer R, Marx I, Guski H, Wenselides K (1979) Morphometric characterization of left ventricular myocardial cells of male rats during post natal development. J Mol Cell Cardiol 11:631–638

Dow JW, Harding NGL, Powell T (1981a) Isolated cardiac myocytes. I. Preparation of adult myocytes and their homology with the intact tissue. Cardiovasc Res 15:483–514

Dow JW, Harding NGL, Powell T (1981b) Isolated cardiac myocytes. II. Functional aspects of mature cells. Cardiovasc Res 15:549–579

Frank JS, Beydler S, Kreman M, Rau EE (1980) Structure of the freeze-fractured sarcolemma in the normal and anoxic rabbit myocardium. Circ Res 47:131–143

Frank JS, Rich TL, Beydler S, Kreman M (1982) Calcium depletion in rabbit myocardium. Ultrastructure of the sarcolemma and correlation with the calcium paradox. Circ Res 51:117–130

Fry DM, Scales D, Inesi G (1979) The ultrastructure of membrane alterations of enzymatically dissociated cardiac myocytes. J Mol Cell Cardiol 11:1151–1163

Geiger B, Tokuyasu KT, Dutton AH, Singer SJ (1980) Vinculin, an intracellular protein localized at specialized sites where microfilament bundles terminate at cell membranes. Proc Natl Acad Sci USA 77:4127–4131

Geiger B, Dutton AH, Tokuyasu KT, Singer SJ (1981) Immunoelectron microscope studies of membrane-microfilament interactions: distributions of α-actinin, tropomyosin and vinculin in intestinal epithelial brush border and chicken gizzard smooth muscle cells. J Cell Biol 91:614–628

Gerdes AM, Kriseman J, Bishop SP (1982) Morphometric study of cardiac muscle. The problem of tissue shrinkage. Lab Invest 46:271–274

Gros D, Potreau D, Mocquard J-P (1980) The myocardial plasma membrane during development: influence of glutaraldehyde fixation on the density and size of intramembranous particles. J Cell Sci 43:301–317

Hatt P-Y, Jouannot P, Moravec J, Perennec J, Laplace M (1978) Development and reversal of pressure-induced hypertrophy: light and electron microscopic study in the rat under temporary aortic constriction. Basic Res Cardiol 73:405–421

Jewell BR (1977) A re-examination of the influence of muscle length on myocardial performance. Circ Res 40:221–230

Jones GE, Severs NJ, Witkowski J (1983) Freeze-fracture analysis of plasma membranes in Duchenne muscular dystrophy. A study using cultured skin fibroblasts. J Neurol Sci 58:185–193

Kordylewski L, Karrison T, Page E (1983) P-face particle density of freeze-fractured vertebrate cardiac plasma membrane. Am J Physiol 245:H992–997

Langendorff O (1895) Untersuchungen am überlebenden Säugetierherzen. Pflügers Archiv 61:291–332

Levin KR, Page E (1980) Quantitative studies on plasmalemmal folds and caveolae of rabbit ventricular myocardial cells. Circ Res 46:244–255

McCallister LP, Trapukedi S, Neely JR (1979) Morphometric observations on the effects of ischaemia in the isolated perfused rat heart. J Mol Cell Cardiol 11:619–630

Nash GB, Tatham PER, Powell T, Twist VW, Speller RD, Loverock LT (1979) Size measurements on isolated rat heart cells using Coulter analysis and light scatter flow cytometry. Biochim Biophys Acta 587:99–111

Nayler WG, Yepez C, Grau A, Slade A (1978) Protective effect of methylprednisolone sodium succinate on the ultrastructure and resting tension of hypoxic heart muscle. Cardiovasc Res 12:91–98

Page E, McCallister LP (1973) Quantitative electron microscopic description of heart muscle cells. Application to normal, hyper-

trophied and thyroxin-stimulated hearts. Am J Cardiol 31:172–181

Page SG (1974) Measurements of structural parameters in cardiac muscle. In: Porter R, Fitzsimons DW (eds) The physiological basis for starling's law of the heart (Ciba Foundation symposium 24) Elsevier, Amsterdam, 13–25

Pardo JV, Siliciano JD, Craig SW (1983a) A vinculin-containing cortical lattice in skeletal muscle: transverse lattice elements ('costameres') mark sites of attachment between myofibrils and sarcolemma. Proc Natl Acad Sci USA 80:1008–1012

Pardo JV, Siliciano JD, Craig SW (1983b) Vinculin is a component of an extensive network of myofibril-sarcolemma attachment regions in cardiac muscle fibres. J Cell Biol 97:1081–1088

Pauli BU, Friedell GH, Weinstein RS (1978) Topography and numerical densities of intramembrane particles in chemical carcinogen-induced urinary bladder carcinomas in Fischer rats. Lab Invest 39:565–573

Powell T, Terrar DA, Twist VW (1980) Electrical properties of individual cells isolated from adult rat ventricular myocardium. J Physiol 302:131–153

Rayns DG, Simpson FO, Bertaud WS (1968) Surface features of striated muscle. I. Guinea-pig cardiac muscle. J Cell Sci 3:467–474

Reith A, Fuchs S (1973) The heart muscle of rat under influence of triiodothyronine and riboflavin deficiency with special reference to mitochondria. A morphologic and morphometric study by electron microscopy. Lab Invest 29:229–235

Robinson TF, Hayward BS, Krueger JW, Sonnenblick EH, Wittenberg BA (1981) Isolated heart myocytes: ultrastructural case study technique. J Microsc 124:135–142

Roos KP, Brady AJ, Tan ST (1982) Direct measurement of sarcomere length from isolated cardiac cells. Am J Physiol 242:H68–78

Severs NJ, Slade AM, Powell T, Twist VW, Warren RL (1982) Correlation of ultrastructure and function in calcium-tolerant myocytes isolated from the adult rat heart. J Ultrastruct Res 81:222–239

Shotton DM (1982) Quantitative freeze-fracture electron microscopy of dystrophic muscle membranes (Review) J Neurol Sci 57:161–190

Stewart JM, Page E (1978) Improved stereological techniques for studying myocardial cell growth. Application to external sarcolemma, T system, and intercalated disks of rabbit and rat hearts. J Ultrastruct Res 65:119–134

Weibel ER (1969) Stereological principles for morphometry in electron microscopic cytology. Int Rev Cytol 26:235–302

Wittenberg BA, Robinson TF (1981) Oxygen requirements morphology, cell coat and membrane permeability of calcium-tolerant myocytes from hearts of adult rats. Cell Tissue Res 216:231–251

Accepted November 5, 1984